Sports Engineering (2018)

Optimization-Based Motor Control of a Paralympic Wheelchair Athlete

Brock Laschowski,[1] Naser Mehrabi,[2] John McPhee[1,2]

[1]Department of Mechanical & Mechatronics Engineering, University of Waterloo, Canada
[2]Department of Systems Design Engineering, University of Waterloo, Canada

Acknowledgments

The authors thank the Paralympian for participating in this research. The authors also recognize the Canadian Sport Institute Ontario and Curling Canada for their support. This research was funded by Dr. John McPhee's Tier I Canada Research Chair in Biomechatronic System Dynamics.

Correspondence Address

Brock Laschowski, Department of Mechanical and Mechatronics Engineering, University of Waterloo, Ontario N2L 3G1, Canada. Email: blaschow@uwaterloo.ca. Telephone: 519-884-4567 ext. 33825

Abstract

The following research approximated how the central nervous system of spinal cord injured Paralympic athletes resolve kinematic redundancies during upper-limb movements. A multibody biomechanical model of a tetraplegic Paralympic athlete was developed using subject-specific body segment parameters. The angular joint kinematics throughout a specified Paralympic sport movement (i.e., wheelchair curling) were experimentally measured using inertial measurement units. The motor control system of the Paralympian was mathematically modelled and simulated using forward dynamics optimization. The predicted kinematics from different optimization objective functions (i.e., minimizing resultant joint moments, mechanical joint power, and angular joint velocities and accelerations) were compared with those experimentally measured throughout the wheelchair curling movement. Of the optimization objective functions under consideration, minimizing angular joint accelerations produced the most accurate predictions of the kinematic trajectories (i.e., characterized with the lowest overall root mean square deviations) and the shortest optimization computation time. The implications of these control findings are discussed with regards to optimal wheelchair design through predictive dynamic simulations.

Keywords

Biomechanics; Control; Dynamics; Modelling; Multibody; Optimization; Paralympics; Redundancy; Simulation; Tetraplegia; Wheelchair

1 Introduction

Motor control is the process through which the central nervous system coordinates multibody movements. Human motor control is exceptionally complex considering the skeletal system is kinematically redundant (i.e., there are more degrees of freedom than required to execute a particular movement). The human skeletal system has 244 degrees of freedom [1]. To position the hand in three-dimensional space, the central nervous system must specify 244 variables, of which 238 are redundant [1]. Dr. Nikolai Bernstein originally identified the inherent kinematic redundancies of multibody human movements in the late 1960s [2]. Nonetheless, biomechanists are still attempting to understand how the central nervous system controls the body's numerous degrees of freedom despite the considerable number of potential solutions.

An emerging area of human movement science involves examining the motor control system of individuals with spinal cord injuries. The spinal cord is a conduit through which motor and sensory information travels between the musculoskeletal and central nervous systems [3]. A spinal cord injury affects the conduction of motor and sensory signals across the sites of lesion, whereby key pathways necessary for signal transmission are disrupted [4]. Typical motor control pathologies following an incomplete spinal cord injury include: tonic physiological responses, spasticity, muscular co-contraction, and inefficient timing of movements [4]. Information regarding how individuals with spinal cord injuries execute multibody movements could provide valuable insights into how the musculoskeletal and central nervous systems interact to control the body.

Biomechanists have used optimization methods to mathematically model and simulate how the central nervous system resolves kinematic redundancies [5-15]. In particular, forward dynamics optimization involves solving the same problem confronted by the central nervous system (i.e., determining the neural excitations that drive multibody movements). The motor control system is represented using a mathematical optimization model, whereby a specified objective function is minimized (or maximized)

subject to constraints. The advantage of this method lies in its predictive capability since it has the potential to mimic the underlying control system. The central nervous system utilizes an unknown algorithm that controls the human body [6, 11-15]. One of the main challenges for biomechanists is choosing a representative objective function for a particular motor task. In situations where the objective is not apparent, forward dynamics optimization could be used to evaluate different objectives to assess which function brings about multibody movements that resemble experimental measurements.

To the best of the authors' knowledge, there has been no previously published research quantifying the underlying motor control system of spinal cord injured Paralympic athletes. Accordingly, the purpose of the following research was to mathematically model and simulate the motor control system of a tetraplegic Paralympic athlete using forward dynamics optimization. The predicted kinematics from different optimization objective functions were compared with those experimentally measured throughout a specified Paralympic sport movement (i.e., wheelchair curling).

2 Methods

2.1 Paralympic Athlete

A single wheelchair curler (sex = male, age = 39 years) was recruited from the Canadian Paralympic Team. The athlete was a gold medalist at the 2014 Winter Paralympic Games and 2013 World Wheelchair Curling Championships. In 2007, the athlete sustained a traumatic incomplete spinal cord injury between the 5^{th} and 6^{th} cervical vertebrae and was diagnosed with tetraplegia. An incomplete spinal cord injury involves preservation of motor and/or sensory function below the neurological level of injury [3]. The athlete was diagnosed with a level "C" impairment on the American Spinal Injury Association Impairment Scale (i.e., an internationally recognized method of categorizing motor and sensory impairments in individuals with spinal cord injuries). The scores range between "A" and "E", wherein A represents a complete spinal cord injury and E represents habitual motor and sensory function. The Paralympian has

significant neuromuscular paralysis in his right hand. Informed written consent from the athlete was obtained and the University of Waterloo Office of Research Ethics approved this research.

2.2 Experimental Kinematics

Angular joint kinematics throughout the wheelchair curling movement were experimentally measured using an inertial measurement unit (IMU) system (MVN, Xsens Technologies, Netherlands). The system consists of 17 IMUs, which were attached to the Paralympian's head, torso, upper arms, forearms, hands, thighs, shanks, and feet. Each IMU contains a triaxial linear accelerometer, rate gyroscope, and magnetometer [16]. The linear accelerometers measure accelerations including the gravitational acceleration, the magnetometers measure the geomagnetic field, and the rate gyroscopes measure angular velocities. The IMU system utilizes a 23-segment biomechanical model and proprietary algorithms to calculate the angular joint kinematics [16]. Previous research has demonstrated the test-retest reliability [17] and convergent validity [18] of the IMU system in computing angular joint kinematics compared with optical motion capture. Following a standard calibration of the IMU system, the Paralympian performed 14 "deliveries" of the curling stone interspersed with 2 minutes of rest between deliveries. Data were sampled at 120 Hz. The goal in wheelchair curling is to push the curling stone with a delivery stick such that the stone rectilinearly translates along the ice over 28 meters and lands within a targeted area. High-frequency noise in the joint kinematic measurements was minimized during post-processing using smoothing splines with MATLAB's default values (MathWorks, USA).

Movement of the curling stone was recorded with a digital camera (Nikon D3100, Nikon Corporation, Japan) that was positioned perpendicular to the Paralympian's plane of motion. The camera sampled at 29 frames per second. The translational stone kinematics (i.e., displacements and velocities) throughout the delivery were determined relative to an inertial reference frame using markerless feature tracking software (ProAnalyst, Xcitex Incorporation, USA). The delivery was defined as the time duration

between the initial displacement of the curling stone and its moment of release from the delivery stick. High frequency noise in the stone kinematic measurements was minimized using smoothing splines with MATLAB's default values (MathWorks, USA).

2.3 Multibody Biomechanical Model

A novel biomechanical model of the wheelchair curling movement was developed using MapleSim software (Maplesoft, Canada). The model consisted of a two-dimensional multibody slider mechanism with a closed kinematic chain (Figure 1). The model included a representative torso, head-and-neck, right upper arm, right forearm, right hand, delivery stick, and curling stone (Figure 1a). The wheelchair was fixed to an inertial reference frame. The mechanical parameters of each biological body segment (i.e., mass, length, center of mass position, and moment of inertia) were experimentally measured using dual-energy x-ray absorptiometry (Table 1) [19-20]. It was assumed that the sagittal plane inertial parameters are comparable with those in the frontal plane, which were experimentally measured using medical imaging [19-20]. From measurements of the Paralympian's equipment configuration, the delivery stick body segment was set to 1.96 m in length, 0.18 kg in mass, and the moment of inertia was calculated using $I_{zz} = \frac{1}{12}mL^2$. The curling stone body segment was given a mass of 19.96 kg and a height of 0.19 m [21]. Non-inertial reference frames were fixed to each rigid body segment.

The model included a representative hip, shoulder, elbow, and wrist, all of which were modelled as revolute kinematic pairs (Figure 1b). The hip, shoulder, and elbow joints permitted flexion-extension while the wrist joint allowed for radial-ulnar deviation, assuming a neutral hand position. The hip joint was set to 0.62 m above the inertial reference frame (i.e., simulating the height of the wheelchair seat). The revolute joints contained angular viscous damping, the quantities of which were obtained from previous research [22-23]. The wrist was modelled as an energetically passive joint to simulate the limited hand functionality of the Paralympic athlete. A prismatic kinematic pair was used to model the contact between the curling stone and ice; rotations about

the vertical axis were omitted. The contact model also included an opposing force vector representative of dry Coulomb friction (i.e., the product of the coefficient of dynamic friction and the normal force) wherein μ = 0.01 [21]; this assumes a constant friction coefficient. The multibody biomechanical model had 3 degrees of freedom and was mathematically represented by 4 ordinary differential equations and 1 algebraic equation (i.e., indicative of the models closed-chain kinematic constraints). The experimental kinematics were mathematically optimized to satisfy the holonomic kinematic constraints of the multibody biomechanical model using a nonlinear constrained optimization algorithm [24].

2.4 Forward Dynamics Optimization

Forward dynamics optimization of the wheelchair curling movement was computed with GPOPS II software, which utilizes direct collocation [25]. Direct collocation converts the model's differential algebraic equations into algebraic constraints by evaluating the system equations of motion at collocation points (i.e., nonlinear programming). Both the "control" and "state" variables were simultaneously approximated with an unknown series of polynomial functions over the total time duration. Following an initial guess, both the order and number of polynomials were iteratively updated through different mesh refinement methods (e.g., increasing the number of polynomials) until the objective function was optimized and the constraints were satisfied [25]. Accordingly, no mathematical integration was required. Previous investigations have used direct collocation to simulate multibody human movements [5, 9, 11-12, 15, 26-27]. The trajectories of both the control variables (i.e., resultant joint moments) and state variables (i.e., kinematics) throughout the wheelchair curling movement were predicted through minimizing each of the following objective functions

$$\left[\tau^{\dagger}_{(t)}, \psi^{\dagger}_{(t)}, \dot{\psi}^{\dagger}_{(t)}\right] = \text{Arg min}\left[\int_{t=0}^{tF} \sum_{i=1}^{3} \tau^{2}_{i(t)}\, dt\right] \quad (1)$$

$$\left[\tau^{\dagger}_{(t)}, \psi^{\dagger}_{(t)}, \dot{\psi}^{\dagger}_{(t)}\right] = \text{Arg min}\left[\int_{t=0}^{tF} \sum_{i=1}^{4} \dot{\theta}^{2}_{i(t)}\, dt\right] \quad (2)$$

$$\left[\tau_{(t)}^{\dagger}, \psi_{(t)}^{\dagger}, \dot{\psi}_{(t)}^{\dagger}\right] = \text{Arg min}\left[\int_{t=0}^{tF} \sum_{i=1}^{4} \ddot{\theta}_{i(t)}^{2}\, dt\right] \quad (3)$$

$$\left[\tau_{(t)}^{\dagger}, \psi_{(t)}^{\dagger}, \dot{\psi}_{(t)}^{\dagger}\right] = \text{Arg min}\left[\int_{t=0}^{tF} \sum_{i=1}^{3} \left(\tau_{i(t)}\dot{\theta}_{i(t)}\right)^{2} dt\right] \quad (4)$$

subject to

$$\psi_{min}^{m} < \psi_{(t)} < \psi_{max}^{m} \quad (5)$$

$$\psi_{(t=0)} = \psi_{tI} \quad (6)$$

$$\psi_{tF}^{lower} < \psi_{(t=tF)} < \psi_{tF}^{upper} \quad (7)$$

$$\begin{cases} \dot{\psi}_{(t)} = f\left(\psi_{(t)}, \tau_{(t)}, \lambda_{(t)}\right) \\ \quad g\left(\psi_{(t)}, \lambda_{(t)}\right) = 0 \end{cases} \quad (8)$$

where τ represented the controls (i.e., resultant joint moments), ψ represented the states (i.e., $\psi = [\theta_1\ \theta_2\ \theta_3\ \theta_4\ x]^T$), x was the modelled displacement of the curling stone, $\dot{\psi}$ were the time derivatives of ψ, ψ^m were the experimentally measured ψ variables, tF was the mean final time (i.e., 0.65 seconds), $\dot{\theta}$ were the angular joint velocities, $\ddot{\theta}$ were the angular joint accelerations, λ was the Lagrange Multiplier, and ψ_{tI} and ψ_{tF} were the state variables at the initial and final times, respectively. The optimization objective functions (i.e., Equations 1-4) were taken from [1, 28-29]. Equation (1) minimized the resultant joint moments, Equation (2) minimized the angular joint velocities, Equation (3) minimized the angular joint accelerations, and Equation (4) minimized the mechanical joint power. Equation (5) specified the minimum and maximum kinematic bounds on each ψ variable. The Paralympian's maximum joint range of motion about the hip (θ_1), shoulder (θ_2), elbow (θ_3), and wrist (θ_4) were experimentally measured using a digital goniometer. Equation (8) represented the multibody system dynamics, which consisted of 4 ordinary differential equations and 1 algebraic equation. The nonlinear programming was solved using an interior point optimizer [30]. The predicted kinematics from the different optimization objective functions were compared with

those experimentally measured throughout the wheelchair curling movement. Examinations of the resultant joint moments are described in [24].

3 Results

Regarding the hip, shoulder, and elbow joints, all the optimization objective functions produced angular displacement trajectories that were in moderate qualitative agreement with the experimental kinematics (Figure 2). Minimizing angular joint accelerations was the only optimization objective function to accurately predict the angular displacements of the wrist joint. As expected, minimizing angular joint velocities produced straight-line angular displacement trajectories between the specified initial and final conditions (Figure 2).

The root mean square deviation (RMSD) of each objective function was calculated to quantitatively assess the agreement between the experimental and predicted joint angles (Table 2). RMSDs are the square roots of the mean squared deviations between the experimental and predicted kinematics; a RMSD of zero denotes perfect agreement. Independent of the objective function being evaluated, the hip joint had the lowest RMSDs, indicating that the forward dynamics optimization consistently and accurately predicted the hip joint angular displacements. Minimizing angular joint accelerations resulted in the lowest overall RMSDs relative to the other optimization objective functions (Table 2).

None of the objective functions predicted angular joint velocities that had sufficient qualitative agreement with the experimental kinematics (Figure 3). Nonetheless, minimizing angular joint accelerations resulted in the smoothest angular velocity trajectories. Minimizing angular joint velocities produced straight-line horizontal kinematic trajectories between the specified initial and final conditions (Figure 3). Minimizing angular joint accelerations resulted in the lowest overall RMSDs relative to the other optimization objective functions (Table 3). Independent of the objective function being evaluated, the forward dynamics optimization was less accurate in

predicting the angular joint velocities compared to the angular displacements. For instance, regarding the elbow joint, the mean percent error of the predicted angular displacements was 13.8 ± 6.5 % whereas the mean percent error of the angular velocities was 27.7 ± 7.8 %; the other joints displayed similar trends.

Aside from minimizing the angular joint velocities, all the optimization objective functions predicted translational stone displacements that were in good qualitative agreement with the experimental kinematics (Figure 4). These findings were quantitatively illustrated through the corresponding RMSDs (Table 4). Though the initial and final conditions of the states (i.e., kinematics) were specified in accordance with the experimental measurements, the final conditions were allocated a range of quantities, which characterized the Paralympian's inter-delivery inconsistencies. Consequently, the predicted translational stone velocities at the moment of release slightly differed from the experimental kinematics (Figure 4). Minimizing angular joint accelerations resulted in the shortest optimization computation time (i.e., 61 CPU seconds), followed sequentially by mechanical joint power (i.e., 269 CPU seconds), resultant joint moments (i.e., 361 CPU seconds), and angular joint velocities (i.e., 1283 CPU seconds).

4 Discussion

The purpose of the present research was to mathematically model and simulate the motor control system of a tetraplegic Paralympic athlete using forward dynamics optimization. The predicted kinematics from different optimization objective functions were compared with those experimentally measured throughout a specified Paralympic sport movement (i.e., wheelchair curling). Although various objective functions could have been utilized in the forward dynamics optimization, the objective functions under consideration (i.e., minimizing resultant joint moments, mechanical joint power, and angular joint velocities and accelerations) have been previously demonstrated to adequately control non-ambulatory multibody movements [1, 28-29]. Minimizing angular joint accelerations produced the most accurate predictions of the kinematic

trajectories (i.e., characterized through the lowest overall root mean square deviations), and the shortest optimization computation time. None of the objective functions precisely simulated the experimental kinematics, and therefore motor control system, of the Paralympic athlete. Recent research of able-bodied individuals reported that multi-objective optimizations, compared to single-objective functions, produced more accurate predictions of the kinematic trajectories during upper-limb reaching movements [7]. Prospective biomechanists should consider investigating multi-objective optimizations to better understand how the central nervous system of Paralympic athletes resolve kinematic redundancies during multibody movements. Considering this research was limited to one participant, additional work is needed to investigate the optimal control objectives of other Paralympic wheelchair athletes to derive non-subject-specific conclusions.

Possessing redundant degrees of freedom might be essential from a human evolutionary perspective. Bernstein [2] suggested that the redundancy of the human musculoskeletal system allows for motor learning to occur, wherein the central nervous system explores the search space of potential solutions before selecting an optimum. Redundant degrees of freedom might enable individuals with spinal cord injuries to retain movement despite neuromuscular paralyses, which correspond with reduced numbers of dynamic degrees of freedom. Computational models of the human motor control system generally include either open-loop or closed-loop control. Open-loop control postulates that the selection of joint kinematic trajectories is pre-planned by the central nervous system prior to movement execution (i.e., feedforward control). Closed-loop control involves online sensorimotor feedback, like visual, proprioceptive, vestibular, and auditory [5, 14-15]. A potential limitation of the present research is the feedforward nature of the motor control model (Equations 1-8). While such a control system can be used to quantitatively evaluate an optimal solution, it cannot infer how the solution is learned. Additional limitations of the computational design include i) assuming two-dimensionality of the wheelchair curling movement (e.g., omitting torso rotations about the vertical axis) and ii) modelling the dynamics of individual biological

elements (e.g., skeletal muscles, tendons, ligaments, and bursae) using resultant joint moments; the implications of these limitations are discussed in [19, 24].

The motor control system of the Paralympic wheelchair athlete was mathematically modelled and simulated using forward dynamics optimization. Forward dynamics optimization also possesses the distinct capability of i) predicting the effects of model parameters on performance outcomes (i.e., sensitivity analyses) and ii) optimizing equipment designs *in silico* to improve performance and/or minimize the risk of musculoskeletal injuries [31]. This approach allows for predictive "what if" simulations, such as "what if the mechanical parameters of the delivery stick (e.g., mass or length) were altered" and "what if the height of the wheelchair seat was changed". At present, the configurations of the delivery stick and wheelchair are generally selected based on the athlete's subjective preferences rather than quantitative analysis. Suppose a biomechanist wanted to maximize the translational stone velocity at the moment of release through optimizing the height of the wheelchair seat. Experimentally, a variety of different seat heights would have to be investigated, and numerous trials per height to account for intra-athlete inconsistencies. Repetitive trials could bring about neuromuscular fatigue, therefore affecting the validity of the experimental findings. Such trial-and-error methods have been recently documented in Paralympic wheelchair rugby [32] and wheelchair basketball [33]. Forward dynamics optimization, by contrast, does not require expensive and time-consuming experiments to attain a solution. Accordingly, the presented multibody biomechanical model (i.e., comprising subject-specific body segments parameters, multibody kinematics, and optimal motor control) could be used to predict the effects of model parameters on Paralympic sport performance and/or optimize equipment designs prior to prototyping.

5. Conclusion

The motor control system of a tetraplegic Paralympic athlete was mathematically approximated using subject-specific biomechanical modelling and forward dynamics optimization. The predicted upper-limb kinematics from different optimization objective

functions were compared with those experimentally measured throughout a specified Paralympic sport movement to determine the objective function most representative of the underlying motor control. It was found that minimizing angular joint accelerations produced the most accurate predictions of the kinematic trajectories and the shortest optimization computation time. Such subject-specific control algorithms can be utilized in predictive dynamic simulations for wheelchair design optimization, reducing the need for numerous time-consuming and expensive experiments by minimizing the search space of potential wheelchair designs.

Conflict of Interest

The authors declare that they have no conflict of interest

References

1. Zatsiorsky VM (1998) Kinematics of human motion. Human Kinetics, USA.

2. Bernstein N (1967) The co-ordination and regulation of movements. Pergamon Press, USA.

3. Kirshblum SC et al (2011) International standards for neurological classification of spinal cord injury (Revised 2011). Journal of Spinal Cord Medicine 34:535-546. doi:10.1179/204577211X13207446293695.

4. Prilutsky B et al (2011) Motor control and motor redundancy in the upper extremity: Implications for neurorehabilitation. Topics in Spinal Cord Injury Rehabilitation 17:7-15. doi:10.1310/sci1701-07.

5. Mehrabi N, Razavian RS, McPhee J (2015) A physics-based musculoskeletal driver model to study steering tasks. ASME Journal of Computational and Nonlinear Dynamics. doi:10.1115/1.4027333.

6. Popovic D, Oguztoreli MN, Stein RB (1995) Optimal control for an above-knee prosthesis with two degrees of freedom. Journal of Biomechanics 28:89-98. doi:10.1016/0021-9290(95)80010-7.

7. Sha D, Thomas JS (2015) An optimisation-based model for full-body upright reaching movements. Computer Methods in Biomechanics and Biomedical Engineering 18:847-860. doi:10.1080/10255842.2013.850675.

8. Shourijeh MS, McPhee J (2014) Forward dynamic optimization of human gait simulations: A global parameterization approach. ASME Journal of Computational and Nonlinear Dynamics. doi:10.1115/1.4026266.

9. Shourijeh MS, Mehrabi N, McPhee J (2017) Forward static optimization in dynamic simulation of human musculoskeletal systems: A proof-of-concept study. ASME Journal of Computational and Nonlinear Dynamics. doi:10.1115/1.4036195.

10. Shoushtari AL (2013) What strategy central nervous system uses to perform a movement balanced? Biomechatronical simulation of human lifting. Applied Bionics and Biomechanics 10:113-124. doi:10.3233/ABB-130075.

11. De Groote F, Kinney AL, Rao AV, Fregly BJ (2016) Evaluation of direct collocation optimal control problem formulations for solving the muscle redundancy problem. Annals of Biomedical Engineering. doi:10.1007/s10439-016-1591-9.

12. Lin YC, Pandy MG (2017) Three-dimensional data-tracking dynamic optimization simulations of human locomotion generated by direct collocation. Journal of Biomechanics. doi:10.1016/j.jbiomech.2017.04.038.

13. Porsa S, Lin YC, Pandy MG (2016) Direct methods for predicting movement biomechanics based upon optimal control theory with implementation in OpenSim. Annals of Biomedical Engineering 44:2542-2557. doi:10.1007/s10439-015-1538-6.

14. Razavian RS, Mehrabi N, McPhee J (2015) A model-based approach to predict muscle synergies using optimization: Application to feedback control. Frontiers in Computational Neuroscience. doi:10.3389/fncom.2015.00121.

15. Mehrabi N, Razavian RS, Ghannadi B, McPhee J (2016) Predictive simulation of reaching moving targets using nonlinear model predictive control. Frontiers in Computational Neuroscience. doi:10.3389/fncom.2016.00143.

16. Roetenberg D (2006) Inertial and magnetic sensing of human motion. PhD Dissertation, University of Twente.

17. Cloete T, Scheffer C (2010) Repeatability of an off-the-shelf, full body inertial motion capture system during clinical gait analysis. Annual International Conference of the IEEE Engineering in Medicine and Biology Society. doi:10.1109/IEMBS.2010.5626196.

18. Zhang JT, Novak AC, Brouwer B, Li Q (2013) Concurrent validation of Xsens MVN measurement of lower limb joint angular kinematics. Physiological Measurement 34:63-69. doi:10.1088/0967-3334/34/8/N63.

19. Laschowski B, McPhee J (2016) Body segment parameters of Paralympic athletes from dual-energy X-ray absorptiometry. Sports Engineering 19:155-162. doi:10.1007/s12283-016-0200-3.

20. Laschowski B, McPhee J (2016) Quantifying body segment parameters using dual-energy x-ray absorptiometry: A Paralympic wheelchair curler case report. Procedia Engineering 147:163-167. doi:10.1016/j.proeng.2016.06.207.

21. Maeno N (2014) Dynamics and curl ratio of a curling stone. Sports Engineering 17:33-41. doi:10.1007/s12283-013-0129-8.

22. Lebiedowska MK (2006) Dynamic properties of human limb segments. In: Karwowski W (ed) International Encyclopaedia of Ergonomics and Human Factors, 2nd edn. CRC Press, USA. 315-319.

23. Rapoport S, Mizrahi J, Kimmel E, Verbitsky O, Isakov E (2003) Constant and variable stiffness and damping of the leg joints in human hopping. ASME Journal of Biomechanical Engineering 125:507-514. doi:10.1115/1.1590358.

24. Laschowski B, Mehrabi N, McPhee J (2016) Inverse dynamics modelling of Paralympic wheelchair curling. Journal of Applied Biomechanics 33:294-299. doi:10.1123/jab.2016-0143.

25. Patterson MA, Rao AV (2012) GPOPS II: A MATLAB software for solving multiple-phase optimal control problems using hp-adaptive Gaussian quadrature collocation methods and sparse nonlinear programming. ACM Transactions on Mathematical Software 41:1-37. doi:10.1145/2558904.

26. Ackermann M, Van Den Bogert AJ (2010) Optimality principles for model-based prediction of human gait. Journal of Biomechanics 43:1055-1060. doi:10.1016/j.jbiomech.2009.12.012.

27. Miller RH, Hamill J (2015) Optimal footfall patterns for cost minimization in running. Journal of Biomechanics 48:2858-2864. doi:10.1016/j.jbiomech.2015.04.019.

28. Hollerbach JM, Suh KC (1987) Redundancy resolution of manipulators through torque optimization. IEEE Journal of Robotics and Automation RA-3:308-316. doi:10.1109/JRA.1987.1087111.

29. Parnianpour A, Wang JL, Shirazi-Adl A, Khayatian B, Lafferriere G (1999) Computation method for simulation of trunk motion: Towards a theoretical based quantitative assessment of trunk performance. Biomedical Engineering: Applications, Basis and Communications 11:27-39.

30. Biegler LT, Zavala VM (2008) Large-scale nonlinear programming using IPOPT: An integrating framework for enterprise-wide optimization. Computers and Chemical Engineering 33:575-582. doi:10.1016/j.compchemeng.2008.08.006.

31. Xiang Y, Arora JS, Abdel-Malek K (2010) Physics-based modeling and simulation of human walking: A review of optimization-based and other approaches. Structural and Multidisciplinary Optimization 42:1-23. doi:10.1007/s00158-010-0496-8.

32. Haydon DS, Pinder RA, Grimshaw PN, Robertson WSP (2016) Elite wheelchair rugby: a quantitative analysis of chair configuration in Australia. Sports Engineering 19:177-184. doi:10.1007/s12283-016-0203-0.

33. Astier M, Weissland T, Vallier JM, Pradon D, Watelain E, Faupin A (2017) Effects of synchronous versus asynchronous push modes on performance and biomechanical parameters in elite wheelchair basketball. Sports Engineering. doi:10.1007/s12283-017-0245-y.

Table 1. Body segment parameters of the Paralympian as experimentally measured using dual-energy x-ray absorptiometry [18-19]. The quantities are presented as arithmetic means ± 1 standard deviation across multiple scans. Segments in the upper-limb are of the right side. The moments of inertia are represented about the center of mass positions, which were determined relative to the proximal endpoint.

Parameter	Head and Neck	Torso	Upper Arm	Forearm	Hand
Length (m)	0.265 ± 0.005	0.588 ± 0.008	0.291 ± 0.005	0.276 ± 0.002	0.123 ± 0.002
Mass (kg)	6.967 ± 0.085	44.616 ± 0.677	3.099 ± 0.192	1.371 ± 0.009	0.396 ± 0.011
Center of Mass (m)	0.1231 ± 0.0025	0.2237 ± 0.0031	0.149 ± 0.002	0.108 ± 0.001	0.022 ± 0.001
Moment of Inertia ($kg \cdot m^2$)	0.1963 ± 0.0102	2.8508 ± 0.0349	0.0238 ± 0.0022	0.0106 ± 0.0002	0.0022 ± 0.0001

Table 2. Root mean square deviations of the predicted joint angles (°) relative to the experimental kinematics. The quantities were presented as arithmetic means over multiple trials with uncertainties expressed as ± 1 standard deviation.

Joint	Joint Moments	Angular Velocities	Mechanical Power	Angular Accelerations
Hip	2.0 ± 0.6	2.4 ± 0.6	2.8 ± 0.7	3.6 ± 0.7
Shoulder	5.8 ± 1.6	28.3 ± 3.0	12.6 ± 2.9	7.6 ± 2.4
Elbow	17.4 ± 3.9	19.9 ± 3.4	6.6 ± 2.0	9.9 ± 3.3
Wrist	23.0 ± 1.6	8.6 ± 1.6	14.9 ± 1.6	2.4 ± 0.8

Table 3. Root mean square deviations of the predicted angular joint velocities (°/s) relative to the experimental kinematics. The quantities were presented as arithmetic means over multiple trials with uncertainties expressed as ± 1 standard deviation.

Joint	Joint Moments	Angular Velocities	Mechanical Power	Angular Accelerations
Hip	19.2 ± 2.8	28.7 ± 4.8	23.0 ± 3.0	26.5 ± 3.4
Shoulder	57.7 ± 4.6	146.5 ± 9.3	77.8 ± 7.7	50.5 ± 5.6
Elbow	108.6 ± 11.6	111.6 ± 8.8	69.8 ± 10.1	64.2 ± 9.9
Wrist	130.0 ± 6.0	44.4 ± 5.7	81.6 ± 4.5	26.1 ± 6.0

Table 4. Root mean square deviations of the predicted translational stone kinematics relative to the experimental measurements. The quantities are presented as arithmetic means over multiple trials with uncertainties expressed as ± 1 standard deviation.

Stone Kinematics	Joint Moments	Angular Velocities	Mechanical Power	Angular Accelerations
Displacement (m)	0.019 ± 0.008	0.148 ± 0.012	0.054 ± 0.012	0.018 ± 0.008
Velocity (m/s)	0.154 ± 0.024	0.809 ± 0.022	0.319 ± 0.023	0.109 ± 0.026

Fig. 1 Schematic of the multibody biomechanical model. The rigid body segments and lower kinematic pairs are presented in (a) and (b), respectively.

Fig. 2 Experimental and predicted joint angles of the hip, shoulder, elbow, and wrist throughout the wheelchair curling movement. The experimental quantities are presented as arithmetic means over multiple trials with uncertainties expressed as ± 1 standard deviation.

Fig. 3 Experimental and predicted angular joint velocities of the hip, shoulder, elbow, and wrist throughout the wheelchair curling movement. The experimental quantities are presented as arithmetic means over multiple trials with uncertainties expressed as ± 1 standard deviation.

Fig. 4 Experimental and predicted translational stone kinematics (i.e., displacements and velocities) throughout the wheelchair curling movement. The experimental quantities are presented as arithmetic means over multiple trials with uncertainties expressed as ± 1 standard deviation.

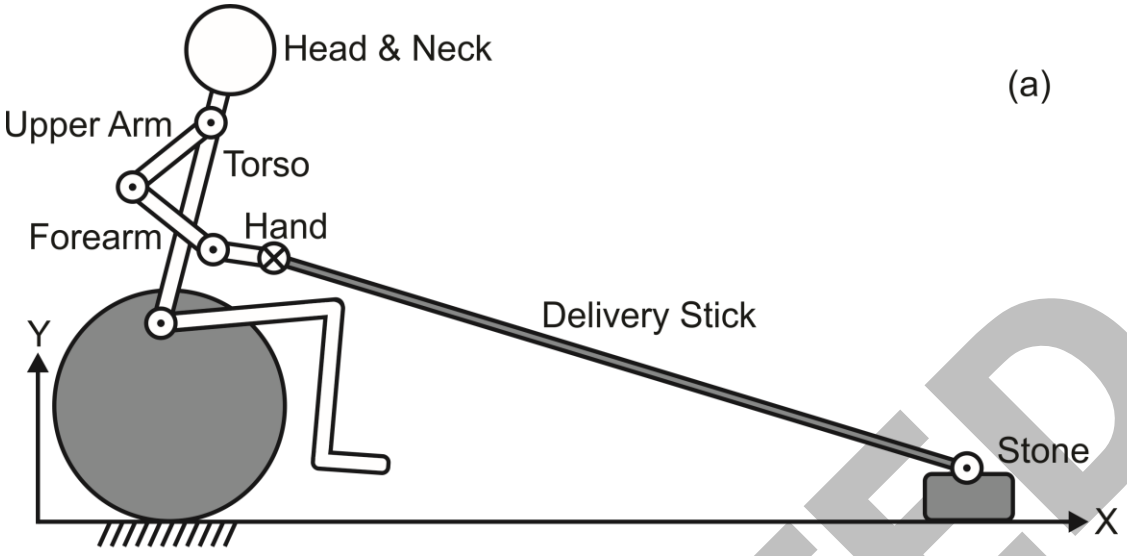
Head & Neck
(a)
Upper Arm
Torso
Forearm
Hand
Delivery Stick
Y
Stone
X

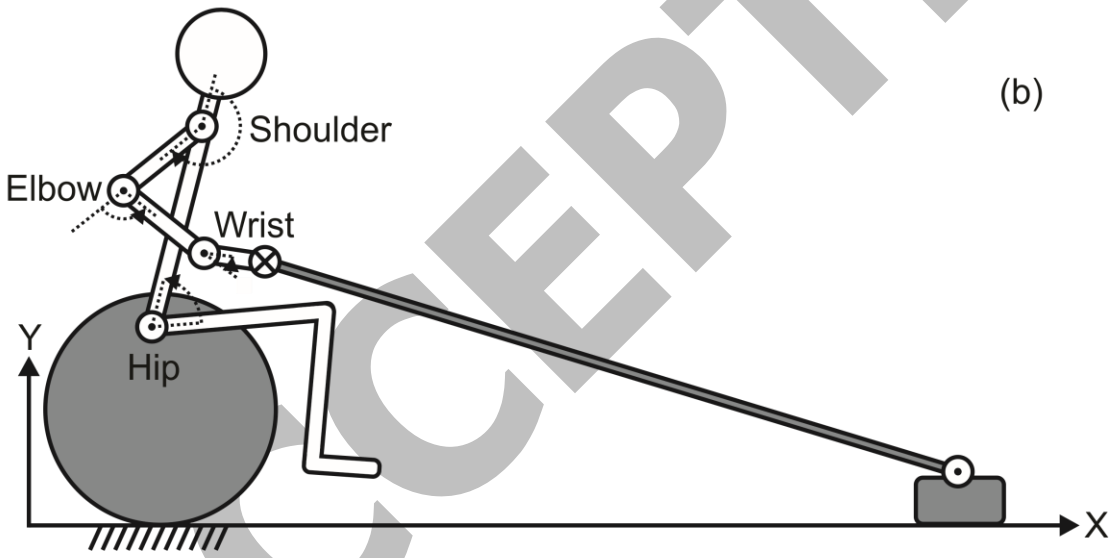
(b)
Shoulder
Elbow
Wrist
Y
Hip
X

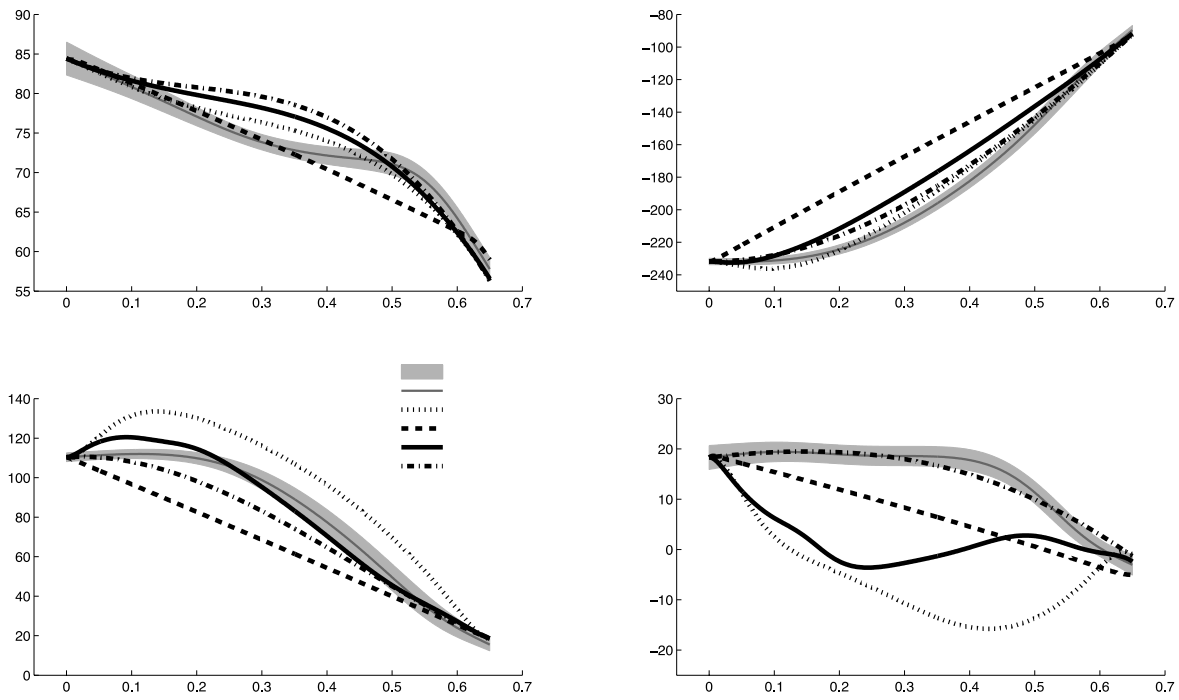
90
85
80
75
70
65
60
55
0 0.1 0.2 0.3 0.4 0.5 0.6 0.7
−80
−100
−120
−140
−160
−180
−200
−220
−240
0 0.1 0.2 0.3 0.4 0.5 0.6 0.7
140
120
100
80
60
40
20
0
0 0.1 0.2 0.3 0.4 0.5 0.6 0.7
30
20
10
0
−10
−20
0 0.1 0.2 0.3 0.4 0.5 0.6 0.7

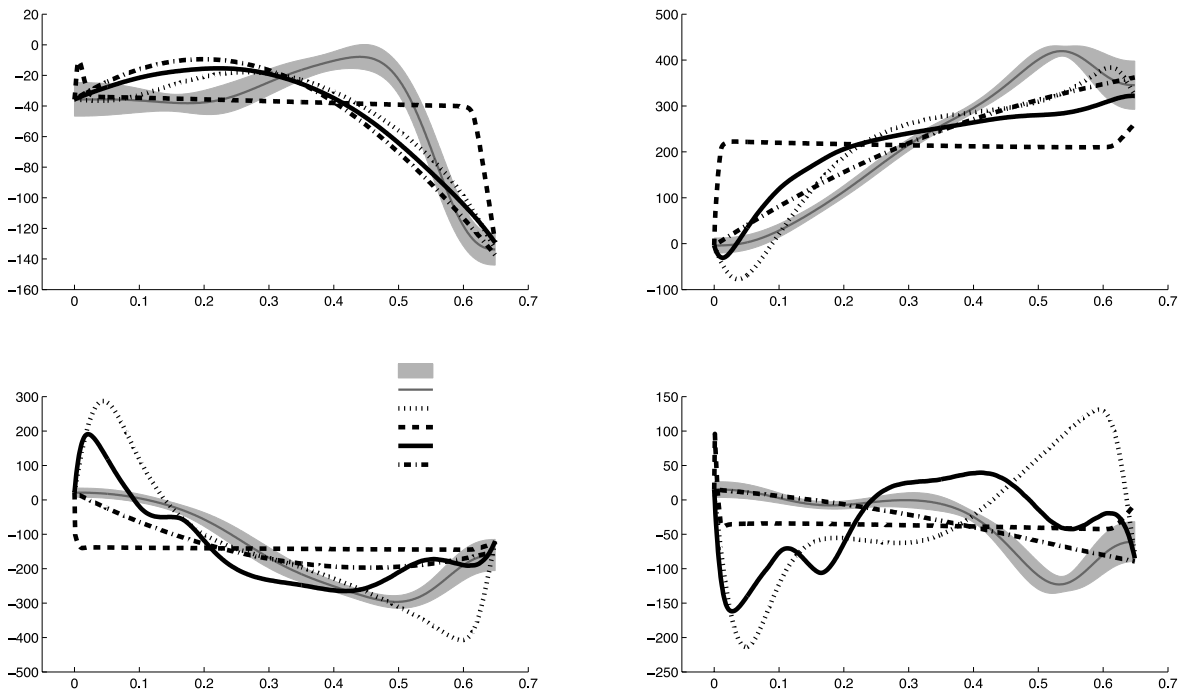
20
0
−20
−40
−60
−80
−100
−120
−140
−160
0
0.1
0.2
0.3
0.4
0.5
0.6
0.7
500
400
300
200
100
0
−100
300
200
100
0
−100
−200
−300
−400
−500
150
100
50
0
−50
−100
−150
−200
−250

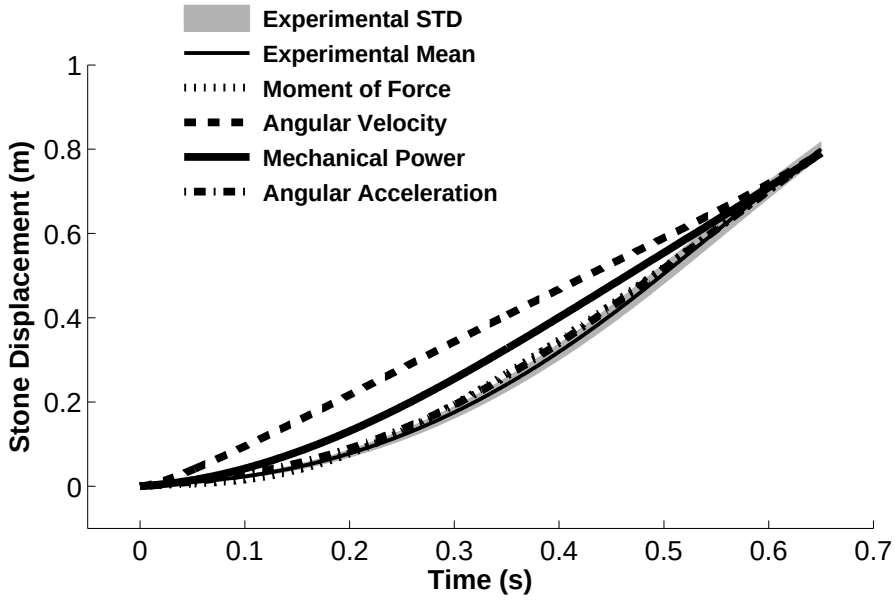
Experimental STD
Experimental Mean
Moment of Force
Angular Velocity
Mechanical Power
Angular Acceleration
Stone Displacement (m)
Time (s)
0
0.2
0.4
0.6
0.8
1
0.1
0.3
0.5
0.7

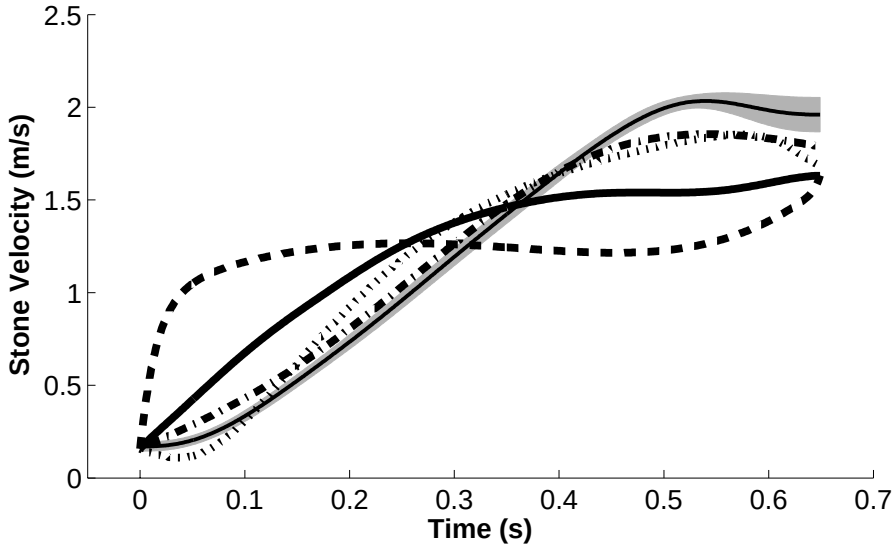
Stone Velocity (m/s)
Time (s)
0
0.5
1
1.5
2
2.5
0.1
0.2
0.3
0.4
0.5
0.6
0.7